

# Systematic Studies of Self-Assembling Peptide Nanofiber Scaffold with Other Scaffolds

Fabrizio Gelain<sup>1,2</sup>, Andrea Lomander<sup>1</sup>, Angelo L. Vescovi<sup>2</sup> and Shuguang Zhang<sup>1,\*</sup>

<sup>1</sup>Center for Biomedical Engineering NE47-379, Massachusetts Institute of Technology, Cambridge, MA 02139-4307, USA

<sup>2</sup>Stem Cell Research Institute, DIBIT, Fondazione Centro San Raffaele del Monte Tabor, Via Olgettina 58, 20132 Milano, Italy

A designer self-assembling peptide nanofiber scaffold has been systematically studied with 10 commonly used scaffolds for several week study using neural stem cells (NSC), a potential therapeutic source for cellular transplantations in nervous system injuries. These cells not only provide a good *in vitro* model of the developing and regenerating nervous system, but also may be helpful in testing for cytotoxicity, cellular adhesion, and differentiation properties of biological and synthetic scaffolds used in medical practices. We tested the self-assembling peptide nanofiber scaffold with the most commonly used scaffolds for tissue engineering and regenerative medicine including PLLA, PLGA, PCLA, collagen I, collagen IV, Matrigel. Additionally, each scaffold was coated with laminin in order to evaluate the utility of this surface treatment. Each scaffold was evaluated by measuring cell viability, differentiation and maturation of the differentiated stem cell progeny (i.e. progenitor cells, astrocytes, oligodendrocytes, and neurons) over 4 weeks. The optimal scaffold should show high numbers of living and differentiated cells. In addition, it was demonstrated that the laminin surface treatment is capable of improving the overall scaffold performance. The designer self-assembling peptide RADA16 nanofiber scaffold represents a new class of biologically inspired material. The well-defined molecular structure with considerable potential for further functionalization and slow drug delivery make the designer peptide scaffolds a very attractive class of biological material for a number of applications. The peptide nanofiber scaffold is comparable with the clinically approved synthetic scaffolds. The peptide scaffolds are not only pure, but also have the potential to be further designed at the molecular level, thus they promise to be useful for cell adhesion and differentiation studies as well as for future biomedical and clinical studies.

**Keywords:** Biologically Inspired Material, Neural Stem Cells, PuraMatrix, Regenerative Medicine.

## 1. INTRODUCTION

Nanoscience and nanotechnology are often associated in materials fabrication, quantum dots, ceramics, electrical engineering, optical devices, microelectronics, microfluidics, and chemical colloid systems. However, nanoscience and nanotechnology have permeated in medical research including regenerative medicine which require two key complementary components:

- (1) a suitable biological scaffold that creates a microenvironment niche for a given cell type, and
- (2) that the given cell type can rapidly integrate and coalesce into the needed tissue.

We here report the use of a class of self-assembling peptide nanofiber scaffold to directly compare with 10 commonly used scaffolds for 4-week study using well-studied neural stem cells (NSC).

The natural capacity of the central nervous system (CNS) to recover from injury is limited,<sup>1,2</sup> thus most research in neurological injuries, including spinal cord injury (SCI), focuses upon promoting axonal growth and reducing neuronal degeneration.<sup>3,4</sup> Multi-potent neural precursors with the capacity to generate neurons, astroglia and oligodendroglia have recently been found in the adult brain and possess the critical features of somatic stem cells. These neural cells not only support neurogenesis within restricted areas throughout adulthood, but also can undergo extensive *in vitro* expansion. Therefore, they have been proposed as a renewable source of neural precursors for regenerative transplantation in various CNS diseases.<sup>5</sup>

Multipotent neural stem cells (NSCs) could enhance neural repair after SCI either by replacing died host cells or, more importantly, through promoting host neurite regeneration. Thus, stem cells could promote axonal regeneration either by reconstituting a “bridge” through a lesion site capable of supporting axonal attachment and

\*Author to whom correspondence should be addressed.

growth or by secreting diffusible molecules, including neurotrophic factors that attract axonal growth cones.

Although the potential medical applications of NSCs are very promising, optimal scaffolds are also needed to accelerate the repair for damaged spinal cord and peripheral nerve lesions. A scaffold is often needed to support the seeded cells. It is also critical to prevent both the scar-tissue formation and fluid-filled tissue gaps that normally result in blockage of growth. These scaffolds need to be harmless, easily manipulated, not to elicit immune responses and biodegradable by cells over time. They should also be a porous scaffold for nerve regeneration and cell repopulation.<sup>6</sup> The reparative and regenerative medicine approach is to

- (1) simulate the architecture of the nervous system via implants consisting of scaffolds seeded with NSCs,
- (2) supports necessary structural cellular organization, and
- (3) direct the growth and the integration with pre-existing circuits within large injury areas.

Although some research has shown the potential of this approach in SCI<sup>7</sup> and brain ischemic injury<sup>8</sup> *in vivo* animal models, few studies have previously been conducted in order to systematically compare scaffolds in cell cultures to systematically evaluate the optimal materials for further animal experiments and future clinical medicine.

In order to use the NSCs for therapies, it is important to first study them with various scaffolds in cell culture studies, which have two advantages:

- (1) a relatively short term analysis of survival and differentiation of heterogeneous substrates optimal as scaffolds for cell transplantation therapies, and
- (2) an effective *in vitro* rapid test for CNS cells for future reparative and regenerative medicine.

We believe that the development of new biological materials is a key area, particularly biologically inspired nanoscale scaffolds mimicking the *in vivo* environment that serve as permissive substrates for cell growth, differentiation and biological function. These materials will not only be useful for furthering our understanding of cell biology in a 3-D environment, but also for advancing medical technology, regenerative biology and medicine.

The ideal biological scaffolds should meet several criteria.

- (1) The building blocks should be derived from biological sources;
- (2) basic units should be amenable to design and modification to achieve specific needs;
- (3) exhibit a controlled rate of material biodegradation;
- (4) exhibit no cytotoxicity;
- (5) promote cell-substrate interactions;
- (6) elicit no or little immune response and inflammation;
- (7) afford economically scaleable material production, purification and processing;
- (8) be readily transportable;

(9) be chemically compatible with aqueous solutions and physiological conditions;

(10) integrate with other materials and in the body.

The objective of our current study is to directly compare 10 commonly used scaffolds with a self-assembling peptide scaffold.<sup>9–16</sup> This is a class of designer biological nanofiber scaffolds also called PuraMatrix (Becton-Dickinson Bioscience, Bedford, MA, USA), particularly promising if used with NSCs in reparative and regenerative medicine approaches for central and peripheral nervous systems.<sup>17</sup>

We here report that the performance of self-assembling peptide scaffold is comparable to other commonly used scaffolds such as poly (DL-lactide acid), poly (lactide-co-glycolide acid 75 : 25 or 50 : 50), poly (capro-lactone acid) and collagen I.<sup>18,19</sup> Although the performance of PuraMatrix was less optimal than other animal derived materials such as collagen IV, fibronectin, laminin and Matrigel mainly used as coatings,<sup>20,21</sup> it nevertheless represents a new class of molecular designer peptide scaffold that fulfills the criteria.

In all cases, additional coating with laminin significantly improved the cell-material interactions of these scaffolds tested. We believe that the molecular-designer peptide scaffolds may have considerable potential for further biological functionalization.

## 2. RESULTS

### 2.1. Scaffold Biodegradation and Cell Attachment

The macroscopic appearance of some of the synthetic scaffolds (PLGA, PCLA, PLLA, PuraMatrix) changed over time. The colour changed from transparent to white opaque, and the initially flat surface of some materials curved during the four weeks of observation. The changes took place at different times for different materials: 2 days for PLLA, 4 days for PLGA (75 : 25), and 7 days for PLGA (50 : 50), which started to fragment after 23 days. This feature could also be observed on substrates seeded with cells (both laminin-coated and uncoated) and each counterpart in controls. This biodegradation time ranking is similar to previously reported results.<sup>22–24</sup> It is known that each experimental design could have important differences related to components of the culture medium used (e.g., enzymes or an acidic environment capable of accelerating the biodegradation processes) and to the scaffold processing adopted, these findings support the fact that we used the standard biomaterial processing procedures.

In each experiment, before each medium change, the pH was measured with a micro pH electrode. However, no significant increase in acidity was observed for these scaffolds, and there was no significant difference in acidity found between the seeded cell samples and the control samples without cells.

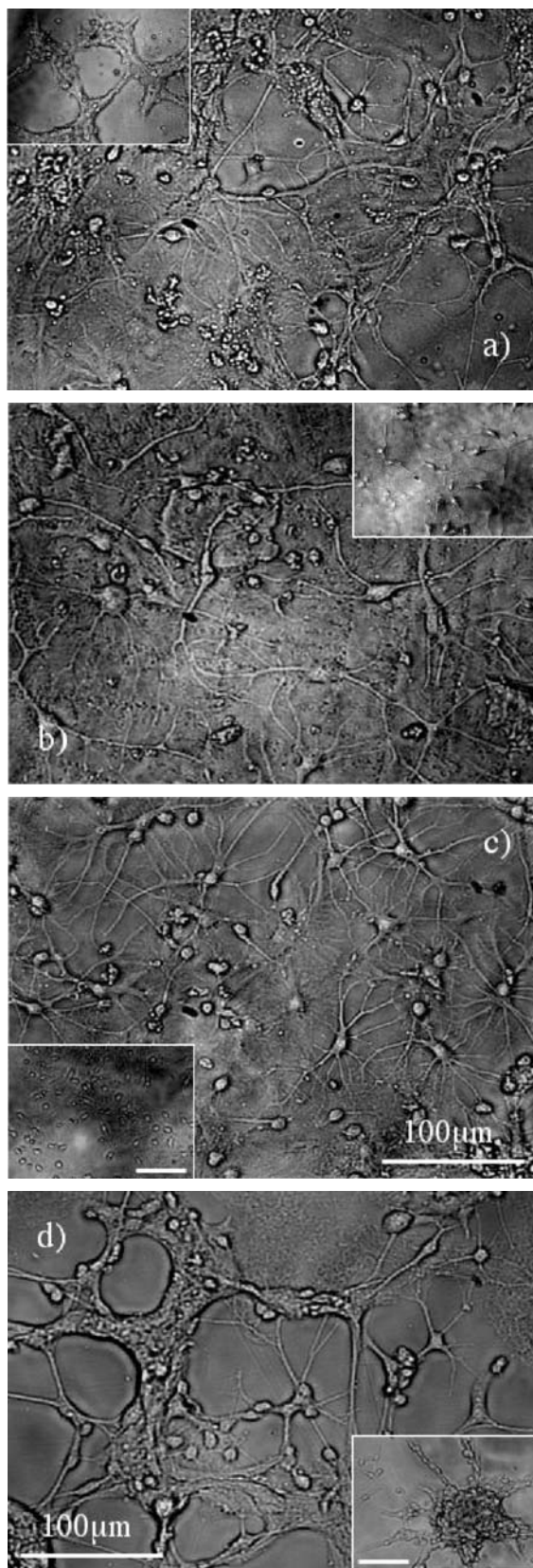


**Fig. 1.** NSCs adhered on different biomaterials 14 days after plating. Phase images of NSCs seeded on PCLA (a), RADA16 (b), collagen IV (c) and collagen I (d). scaffolds alone (small boxes) show poor cell

Based on a systematic analysis of different scaffolds, our experiments allowed us to evaluate different degrees of NSC attachment clearly visible with an inverted optical microscope (Fig. 1). In our observations, Matrigel exhibited the most rapid cell adhesion process and the most extensive cell branching. Laminin and lc-collagen IV (lc represents laminin coated) exhibited comparable cell adhesion and branching as Matrigel. During the course of 7 days, no appreciable differences in the morphology of adhering and differentiating cells were found between the peptide scaffold PuraMatrix and PCLA, PLLA, PLGA (50:50), PLGA (75:25).

After the first week, lc-PCLA and lc-PuraMatrix appeared to be the most preferred biopolymer scaffolds for cell adhesion and branching. On the fibronectin substrate, surprisingly, NSCs formed cell clusters and, after approximately 7 days, cells crossed the entire surface. Cell attachment to the biopolymer scaffolds was greater than the attachment observed on fibronectin; however, the cell attachment for the microfiber scaffolds was less than that on the collagen IV and coated PuraMatrix. However, the cell attachment remained the poorest in collagen I scaffold throughout the course of the study. Cell aggregations resembling the shape of neuro-spheres were also observed. In all cases, a laminin coating dramatically improved the capability of the NSCs to branch, spread and uniformly cover the substrates.

## 2.2. NSCs Long-Term Survival on the Nanofiber Scaffold and Other Scaffolds

The long-term cell survival on each scaffold was evaluated via an MTT assay. The results were obtained from duplicate experiments (Fig. 2). Matrigel and laminin show similar levels in cell population after seeding (5 fold increase after 4 weeks). There was a noticeable proliferation after 1 day of plating due to the medium used (see methods for details). The cells uniformly covered the 1 cm<sup>2</sup> surface area of the tested substrates by the end of 4 weeks. Among the other biomaterials, the lc-collagen IV showed the highest cell survival and proliferation. On the other hand, fibronectin, a commonly used substrate for adhesion cultures,<sup>25</sup> initially showed less cell proliferation. However, by the end of the study, maintenance of the total amount of adherent cells observed on the fibronectin. lc-collagen I appeared to be comparable to fibronectin. The remaining coated scaffolds,

Continued.

adhesion and spreading. Cell clusters are shown with PCLA (a-small box) and clusters morphologically similar to neurospheres with collagen I (d-small box). The coating procedure with laminin dramatically improves the adhesion of cells and branching in all of the materials used (small boxes). Extensive cell branching and spreading with lc-collagen IV (c-big box), branched and bipolar (immature) cell shapes with lc-RADA16 (b-big box). The scale bars in all images are 100 μm.

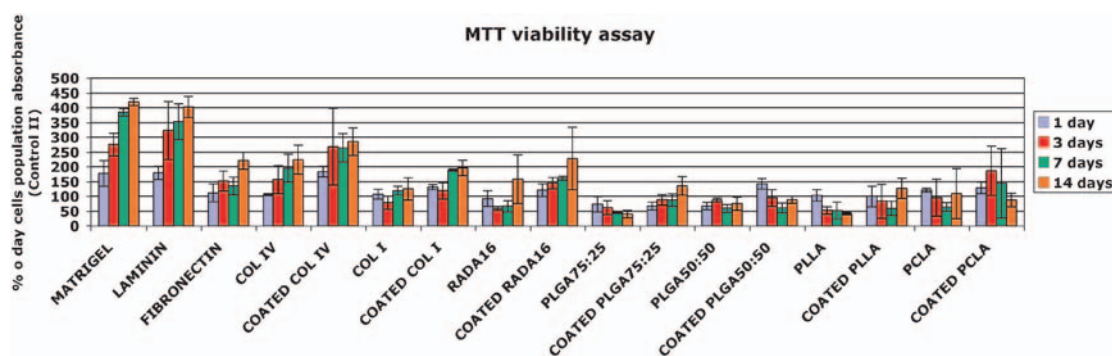


**Fig. 2.** NSCs viability at 1, 3, 7, and 14 days after plating. MTT formazan formation by NSCs seeded on different scaffolds and absorbance measurements. Results are expressed as percentage of the corresponding initial population control II (cells seeded on Matrigel coated wells right before each multi-well plating and tested 2 hours after plating) and are expressed as means  $\pm$  STD ( $n = 2$ ). Uncoated polymer scaffolds showed a decrease of the initial cell population seeded over time. Matrigel, laminin and lc-collagen IV allow long-term (four weeks) cell proliferation and survival. Note that the results of lc-RADA16 (PuraMatrix) are comparable to fibronectin, lc-collagen I and all the coated scaffolds tested (lc-PLLA, lc-PCLA, lc-PLGA 75 : 25, lc-PLGA 50 : 50). These cultures were also kept for 28 days (results not shown).

lc-PuraMatrix, lc-PCLA, lc-PLLA, lc-PLGA (50 : 50) and lc-PLGA (75 : 25) showed similar results: no significant increase in cell population was observed, but the original population seeded was maintained except for lc-PLGA (50 : 50) and lc-PLLA ( $\sim 20\%$  decrease).

By comparing the scaffolds tested with and without coating, the surface treatment with laminin produced a general increase in cell survival in the long-term cultures. For example, coating RADA16 resulted in a 3-fold

increase and coating collagen IV resulted in a 2-fold increase in cell survival. Interestingly, in the cases of biopolymer scaffolds without surface treatment, the cell population decreased to below half of the initial seeding. When ranking the cell survival results for both the set of coated scaffolds and the set of uncoated scaffolds, the same order results, which suggest a consistent influence of the original scaffolds (even after the coating treatment) on cell adhesion and proliferation (Fig. 6).

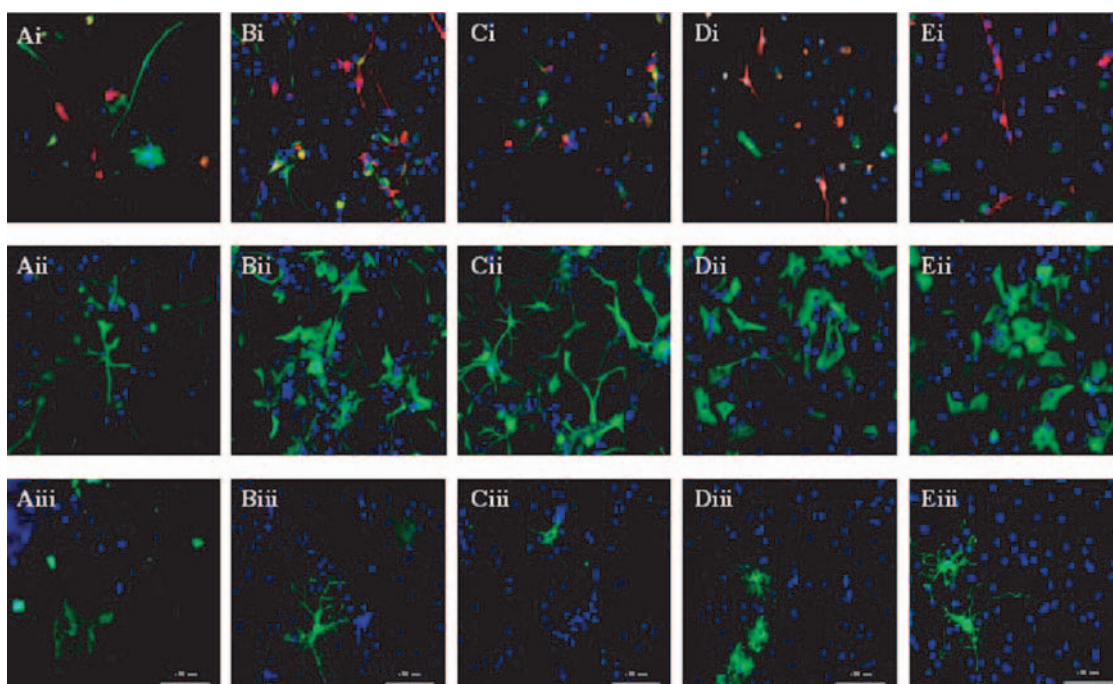


**Fig. 3.** NSCs differentiation and maturation 14 days after plating. NSCs seeded on lc-PuraMatrix (A column), lc-PCLA (B column), lc-collagen I (C column), lc-collagen IV (D column) and Matrigel (E column). Cell nuclei were stained in blue with the nucleic acid stain DAPI. In the first row, NSCs were stained for a progenitor marker (Nestin<sup>+</sup> in green) as well as a neuronal marker ( $\beta$ -Tubulin<sup>+</sup> in red). The presence of GFAP<sup>+</sup> and Galactocerebroside<sup>+</sup> markers were also tested in order to detect, respectively, astrocytes (second row in green) and oligodendrocytes (third row in green). Cell concentration is variable due to both cell survival and irregularities in the biomaterial surfaces. Neurons and astrocytes showed different morphologies ranging from bipolar and multipolar immature shapes (A and C), to extensively branched and spread cells (B, D, and E). Oligodendrocytes as well look significantly branched in B, D, and E. Scale bars 100  $\mu$ m.

### 2.3. NSCs Differentiation on the Diverse Scaffolds

NSCs differentiation was evaluated at days 7 and 14 after seeding. Figure 3 shows 14 days after plating with staining of NSCs, seeded on laminin coated scaffolds including lc-PuraMatrix (A i, ii, iii), lc-PCLA (B i, ii, iii), lc-collagen I (C i, ii, iii), lc-collagen IV (D i, ii, iii), and Matrigel (E i, ii, iii). At every time interval, neuronal and glial phenotypes were present with all scaffolds examined. Additionally, as shown in Figure 3 (first row, cells labeled in green), nestin positive cells (Nestin<sup>+</sup>) were detected in all biomaterials.

In the case of Matrigel culture, cells exhibited a regular mature shape with neuronal and oligodendro-glial branching, and showed few numbers of progenitor cells but large numbers of spread astrocytes. On lc-collagen IV culture, astrocytes appeared less mature: some of them in a star shape and with less extensive spreading. This phenomenon increased for lc-PuraMatrix, lc-PCLA, and lc-collagen I (cells labeled in green in row ii). As expected, in the same order, there was an increase in the percent values of Nestin<sup>+</sup> cells (green in row i) and a decrease of

$\beta$ -Tub<sup>+</sup> cells branching (red in row i). No cross-reactivity was observed between these two labeled cell populations: i.e., no yellow labeling (red and green) in row i of Figure 3. Oligodendrocytes appeared to be less influenced by the biomaterials. However, a degree of extended cell branching similar to that found in Matrigel culture was observed on lc-PCLA culture.

$\beta$ -Tub<sup>+</sup> cells, presumably neurons, appeared to grow and adhere on the spontaneously formed glial layer, similar to previous findings of other studies<sup>26,27</sup> and in the case of 2-dimensional growth cultures (Petri dishes or multi-wells).

Quantitatively, Nestin<sup>+</sup> cells generally decreased in all cases as time after plating increased (Fig. 4(a)). However, there was a dramatic difference between the percentage of Nestin<sup>+</sup> cells found on Matrigel, laminin between 4%–11.5% and the rest of the other biomaterials studied here between 7%–32%. lc-collagen IV showed the lowest percentage of Nestin<sup>+</sup> cells between the remaining substrates from 7% to 16%. Most of the scaffolds had similar percentages of immature cells (~15%) 28 days after seeding. However, some important differences appeared during

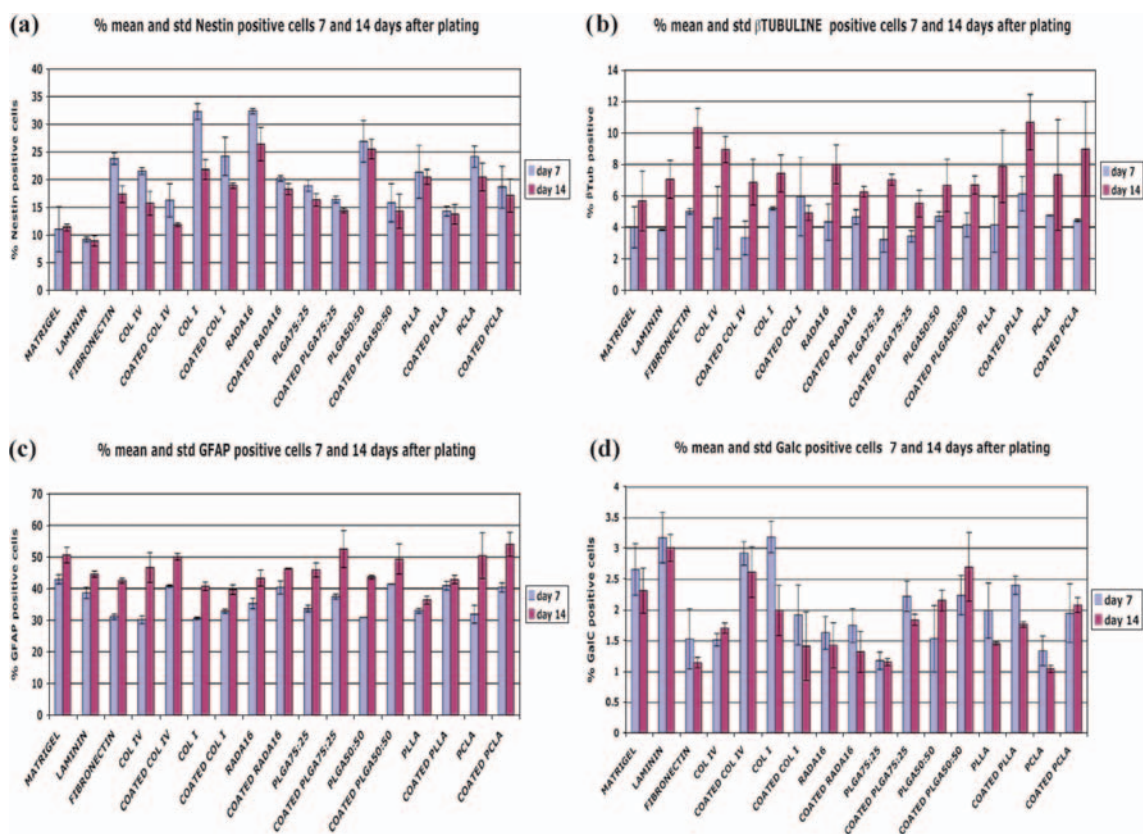


**Fig. 4.** NSCs differentiation at 7 and 14 after plating. NSCs quantitative staining assay for Nestin<sup>+</sup> (a),  $\beta$  Tubulin<sup>+</sup> (b), GFAP<sup>+</sup> (c), and Galactocerebroside<sup>+</sup> (d) cells. We counted 300–900 cells/well depending on cell concentration in 4–15 non-overlapping fields that were randomly chosen to perform the quantitative analyses. Results are expressed as means  $\pm$  STD ( $n = 2$ ). Nestin<sup>+</sup> cells appear to still be significantly present (>10%) 28 days after plating on all the scaffolds except for Matrigel, laminin, and lc-collagen IV. Values of Nestin<sup>+</sup> cells are even higher if the coating treatment is not applied. These uncoated substrates show the highest percentages of Galactocerebroside<sup>+</sup> cells. The percentage of neurons does not appear to be favoured by any particular substrate over time except for lc-PCLA, lc-PLLA, and Matrigel. Astrocytes, the percentage of which increased with time, inversely mirror the Nestin<sup>+</sup> trend in all cases. RAD16 appeared fully comparable to the other synthetic scaffolds PCLA, PLLA, PLGA 75 : 25, and PLGA 50 : 50. These cultures were also kept for 28 days (results not shown).

the first week: fibronectin and lc-collagen I still had 24% immature cells, while lc-collagen IV, lc-PCLA, lc-PLLA, lc-PLGA (75:25) and lc-PLGA (50:50) all had 15% of Nestin<sup>+</sup> cells. In addition, all of the uncoated biomaterials showed a higher percentage of Nestin<sup>+</sup> cells (an increase from ~2% to ~12%), a difference that remained throughout the entire period of experimental observation.

In contrast, GFAP positive cells (GFAP<sup>+</sup>), presumably glia cells, increased over time, yielding the highest percentage for Matrigel and the lowest for fibronectin (Fig. 4(c)). Also, the ranking of the scaffolds for GFAP<sup>+</sup> cells is the reverse of the ranking based on Nestin<sup>+</sup> staining, as expected. Except Matrigel culture, lc-collagen IV culture showed the highest percentage of GFAP<sup>+</sup> cells. The only exception is the case of lc-PLGA (50:50), where the GFAP<sup>+</sup> percentage value is very similar to that of lc-collagen IV, but morphologically the stained cells appeared smaller and in clusters (similar to immature cells with a small round shape) in the first case. They spread and flattened (mature). All of the other scaffolds showed lower values of GFAP<sup>+</sup> glial cells. The coating treatment seemed to contribute to an increase from 1% to 10% in the GFAP<sup>+</sup> cells on all the tested substrates.

$\beta$ -Tubulin staining revealed 8%–12% of  $\beta$ -Tub<sup>+</sup> cells. Matrigel, fibronectin, lc-PCLA, lc-PLLA and lc-PLGA (50:50) (Fig. 4(b)) did not exhibit an important long-lasting increase or decrease over time, nor a particular influence of the coating with laminin. The percentage of Galactocerebroside positive cells (GalC<sup>+</sup>) slightly decreased on almost all the scaffolds studied by the end of the experiments. Additional studies will be carried out to clarify this observation. It should be noted that Matrigel, laminin, and lc-collagen IV showed the highest value of GalC<sup>+</sup> cells. The coating treatment slightly increased the

oligodendroglial population except for collagen I where a high number of oligodendrocytes were found inside clusters (almost neuro-spheres) of cells. The cell clusters almost disappeared on lc-collagen I, suggesting some favorable differentiating environment (other neural cell membranes), because oligodendrocytes was not as prevalent on the lc-collagen I.

#### 2.4. AFM Imaging to Cell-Material Interaction

We also examined NSC differentiation seeded on the scaffolds using AFM. Images of 100  $\mu\text{m}^2$  surfaces were collected, showing

- (1) cells adhered on scaffolds,
- (2) cell clusters, or
- (3) scaffolds alone.

To estimate micro/nano-scale interactions between cells and biomaterials, images of 10  $\mu\text{m}^2$  and 5  $\mu\text{m}^2$  were examined. Both thickness and heights of the biomaterials, cells and overlapping branches (scale in Fig. 5(a)) were imaged. At high resolution, it was possible to detect micro-scale structures of the tested scaffolds, and, qualitatively, to study the morphological interactions between differentiating cells and the scaffolds on which the cells adhered.

In particular, Figure 5(a) shows NSCs differentiated for 7 days on PuraMatrix. In the high magnification area marked with a white rectangle, which focuses on cell branches (Fig. 5(b)), the porous structure of the scaffold, from 5 nm to 200 nm pore size, is visualized.<sup>9–11</sup> Additionally, cell protrusions penetrated into the matrix showing branches with hollow shapes above them, suggesting an intimate interaction between the cells and the nanofiber scaffold PuraMatrix.

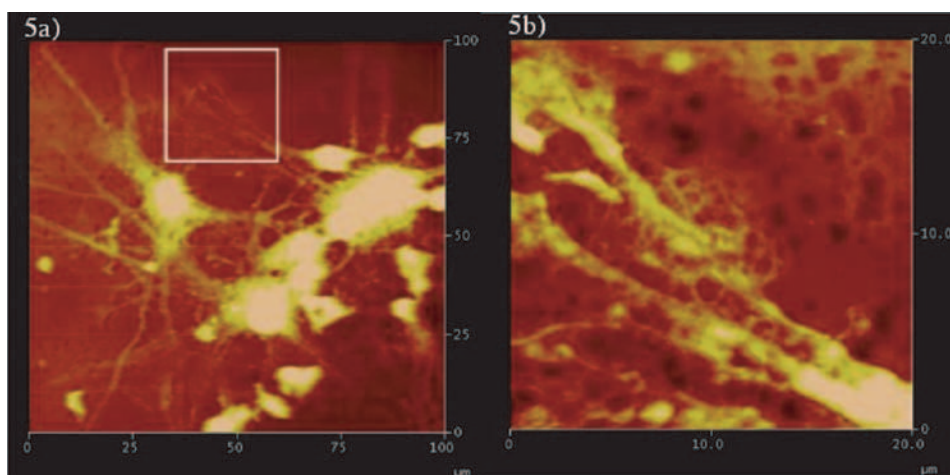


**Fig. 5.** AFM imaging of NSCs and their branches on PuraMatrix. Atomic Force Microscope images of NSCs differentiated for 7 days *in vitro* on PuraMatrix. Large field imaging (a) with 0  $\mu\text{m}$  to 2  $\mu\text{m}$  height brown-scale and higher magnification of the image inside the white box (b) with 0 nm to 450 nm height brown-scale. Large field images are required to find adhering cells, clusters, and branches of interest. In high magnification images, it is possible to estimate scaffold nanostructures (a loose mesh in case of the scaffold) and interactions between cells and scaffolds. Particularly, in (a), it is easy to detect important adhesion contact points of cell branches anchored to and submerged within the scaffold (pore shaped structures overlapping cells).

### 3. DISCUSSION

Our systematic study of a diverse group of scaffolds concerns NSC adhesion, survival, and differentiation. Self-assembling nanofiber scaffold<sup>9-16</sup> is directly compared with several commonly used scaffolds used in regenerative medicine.

We here introduced a series of experiment designs that constitute a useful methodology capable of providing *in vitro* standard quantification of cell adhesion, branching, and differentiation on chemically different scaffolds (but tailored to be physically similar). We significantly reduced the undesired effects related to the scaffold consistency and stiffness by a reliable methodology. We also demonstrated that coating these scaffolds with laminin could not only significantly improve NSC survival but also differentiation and maturation over time.

There are several notable observations. First we observed that astrocytes and progenitor cells were most influenced by the laminin coating and by the scaffolds themselves. Thus, it is plausible that progenitor (Nestin<sup>+</sup>) cells were mainly composed of glial lineage restricted multi-potent cells in our experimental model. This possibility was supported from the observation of the numbers of GFAP<sup>+</sup> and Nestin<sup>+</sup>, and by absence of staining cross-reactions between Nestin<sup>+</sup>,  $\beta$ -Tub<sup>+</sup> and GalC<sup>+</sup>.

Second, our study suggested the spontaneous formation of a glial layer from the NSCs. In most of the cases, under neurons and oligodendrocytes, there was a layer that limited possible influences between membrane receptors of these cell phenotypes and the scaffolds. As a consequence, in 2-D culture conditions, the laminin coated scaffolds seem to mainly influence both the numbers of immature progenitor cells and astrocytes detected, and as a secondary effect (i.e., in a less sensitive way) the percentages of the other phenotypes.

Cells in scaffolds of laminin and I-collagen IV showed cell survival and differentiation closest to Matrigel. Others reported<sup>28,29</sup> a supramolecular assembling between laminin and collagen IV, two major components of basement membranes found in nervous tissues, through a biological cross-linker molecule, nidogen, present in most of the commercially available laminin solution products. However, collagen IV and laminin are coatings without a 3-D macromolecular structure. They are difficult to tailor functional motifs into the scaffolds, but using de-cellularized vein as a source for collagen IV and laminin scaffolds.<sup>30,31</sup> Laminin appears from our results to be the best alternative to Matrigel. However, a chemical modification necessary to obtain a tailor-made 3-D macrostructure is likely to affect the protein molecular structure of laminin, thus altering its binding domain exposure (as well as related molecular structure cascade reactions) to cell adhesion membrane receptors and decreasing its efficiency in promoting cell adhesion and survival.

Collagen I used for neural tissue regeneration<sup>32,33</sup> is an animal derived-scaffolds that showed poor cell adhesion and differentiation in our current study using NSCs. Although the laminin coating improved it, resulting in cell survival and differentiation similar to that of fibronectin, the long-term, partial differentiation still remains an important issue for regenerative medicine applications with NSCs seeded on both of these two animal derived scaffolds.

PLLA, PCL, PLGA (50 : 50), PLGA (75 : 25) scaffolds showed poor cell proliferation maintenance and insufficient cell survival in absence of a laminin surface coating. This may be due to the fact that these synthetic biomaterials lack cell adhesion sites, whereas naturally derived materials contain biological adhesion proteins such as fibronectin<sup>34,35</sup> and laminin.<sup>36,37</sup> This also may be due to the absence of many other secondary molecules, such as growth factors. As a consequence, these scaffolds produced a long-term cell maintenance, temporary NSC proliferation and improved cell attachment when coated with laminin. Particularly, I-c-PCL showed important long-term cell survival and neuronal cell differentiation, up to ~10.5%, probably due to the fact that PCL had the longest biodegradation time with the smallest amount of biodegradation products released. On the other hand, because of the ease in which synthetic scaffolds can be processed, a composite material containing PCL, collagen IV and laminin may be a alternative for cell attachment and scaffold design.

NSCs adhered and differentiated to a similar degree (compared to the other biopolymer scaffolds) on the nanofiber PuraMatrix. With a substrate coating treatment, a significantly improved long-term cellular integration and differentiation is achieved. This new class of designer peptide scaffolds including PuraMatrix may have a great potential to further advance reparative and regenerative medicine. It is not only straightforward to design a wide range of tailor-made scaffolds specifically to introduce functional motifs (and our work suggests to choose from laminin and collagen IV derived motifs), but also to directly incorporate proteins, such as neurotrophic factors. In addition to its ECM like nanostructure capable of wrapping cell bodies and branches (as shown with AFM imaging), these further molecular modifications could lead to an improvement in cell adhesion, migration and the selective promotion of neuronal differentiation in a 3-dimensional environment.<sup>11, 17</sup>

It is commonly known that many scaffolds are benign in the polymer form before degradation. However, the degradation products of some scaffolds cause tissue damage, toxicity and inflammatory concerns. In our experiments, we did not observe a substantial increase of acidity in the media. It is likely that with our protocol the acidity from biodegradation processes is minimized, but the acid products released by PLLA, PLGA (50 : 50), PLGA (75 : 25),

and PCLA could be a concern in animal studies and human clinical therapies. However this would not likely be a concern with scaffolds made of pure amino acids including synthetically designer peptide scaffolds.

## 4. CONCLUSIONS

Neural stem cells are a good model for *in vitro* study of the development and regeneration of the nervous system. They are easy to expand and have been fully characterized. They will be a very useful source for cell-based therapies.<sup>38–40</sup>

Our comprehensive and systematic study not only quantitatively evaluated how NSCs interact with several common scaffolds used in reparative and regenerative medicine, but also provided a framework for further modifications of scaffolds to improve cell survival and differentiation. For example, while polymer scaffolds are easy processing in high purity, they need to be functionalized (or coated) with naturally derived motifs (or proteins) for effective NSC based applications.

Moreover, our *in vitro* study provided important information concerning the ability of the biomaterials studied to support attachment and differentiation of NSCs and other stem cells before starting with time consuming and expensive *in vivo* models for different tissue pathologies.

This is our first step for 2-dimensional biomaterial studies using NSCs. However, a 3-dimensional *in vitro* approach with different cell types and with designer scaffolds will be carried out to closely mimic the *in vivo* physiological scaffolds of interest. Our systematic studies of diverse scaffolds will likely have an impact in many fields including the development of new biological materials and biotechnologies with the aim of pursuing the strategy of cell based reparative and regenerative medicine to overcome pathologies in the central nervous systems.

## 5. METHODS

### 5.1. Scaffolds Fabrication and Coating

In order to both guarantee the reproducibility of our experiments and choose scaffolds commonly used in tissue engineering, we only tested commercially available scaffolds and tailored them following the protocols included in their datasheets (when provided) or protocols already used in the literature.

All of the substrates show 1 cm<sup>2</sup> surface area per well (24 multi-well plate, Linbro, Aurora Ohio) for testing cell adhesion.

*Matrigel* GF-reduced (from EHS sarcoma, Beckton Dickinson Biosciences, Bedford MA) that showed interesting results in SCI regeneration tests.<sup>41</sup>

Diluted 1 : 100 in basal medium poured at 30  $\mu$ l/well 30' incubation at 37°, rinsing and drying under laminar hood for 1 hour. This substrate was chosen as a positive control for NSC adhesion and differentiation.<sup>42</sup>

*Laminin* (mouse from EHS sarcoma, Roche, Penzberg Germany) one of the major components of basal membranes in peripheral and central nervous systems. As suggested by the laminin datasheet: diluted 1 : 5 in PBS 1X PH 7.4, poured at 30  $\mu$ l/well in order to have 3  $\mu$ g/cm<sup>2</sup> final concentration, 45' incubation at 37°, rinsing 3 times with PBS (PH 7.4) and drying under laminar hood for 1 hour.

*Fibronectin* (from human plasma, Sigma, St. Louis, Missouri), already used in combination with NSCs to promote neural regeneration in lesioned mouse brains.<sup>43</sup> From datasheet, diluted 1 : 8 in PBS, poured at 30  $\mu$ l/well in order to have 3.75  $\mu$ g/cm<sup>2</sup> final concentration, 45' incubation at 37°, rinsing 3 times with PBS and drying under laminar hood for 1 hour.

*PLLA* (Poly(DL-lactide), Sigma), *PLGA* 75 : 25 (Poly(DL-lactide-co-glycolide) blend 75%, 25%, Sigma), *PLGA* 50 : 50 (Poly(DL-lactide-co-glycolide) blend 50%, 50%, Sigma), *PCLA* (Poly(DL-Lactide-co-caprolactone) blend 86%, 14%, Aldrich), each of which has been used in countless applications as easily processed scaffolds for nervous system regeneration.<sup>7, 44</sup>

In order to produce thin films, all of the polymers were dissolved in a 5% (wt/vol) solution of Methylene Chloride, then the solutions were poured on glass slides and the solvent was allowed to evaporate into a vacuum desiccator for 2 hours.<sup>45</sup> Then films were detached, rinsed 3 times in PBS to wash away any solvent residue, dried in the laminar hood for 1 hour and cut into 1 cm<sup>2</sup> pieces.

*Collagen I* (from rat tail, Beckton Dickinson Biosciences) recently used for bridging 0.30 mm nerve defects<sup>32</sup> and other nerve regeneration related applications. Following the datasheet gelation procedure: diluted 1 : 5 (24  $\mu$ g/cm<sup>2</sup>) in 0.46% (vol/vol) of 1 N NaOH solution. The contents were mixed in ice cold tubes, poured at 30  $\mu$ l/well and allowed to gel at 37° for 2 hours, rinsed 3 times with PBS to wash away any acid residue (coming from the collagen storage solution) and dried in laminar hood for 1 hour.

*Collagen IV* (mouse from EHS sarcoma, Beckton Dickinson Biosciences), one of the major components of basal membranes in peripheral and central nervous systems. From its datasheet, diluted 1 : 2 (15  $\mu$ g/cm<sup>2</sup>) in 0.05 N HCl solution. The contents were mixed in ice cold tubes, poured at 30  $\mu$ l/well and allowed to gel at 37° for 1 hour, rinsed 3 times with PBS to wash away any acid residue and dried in laminar hood for 1 hour.

*RADA16* self-assembling peptide nanofiber scaffold (PuraMatrix). This biological scaffold consists of greater than 99% water content (peptide content 1–10 mg/ml) when in an aqueous environment. It forms a scaffold when the peptide solution is exposed to physiological media or salt solution. The components of the scaffold consist of amphiphilic peptides that have alternately repeating units of positively charged arginine and negatively charged

aspartic acid (Ac-RADARADARADARADA-CONH<sub>2</sub>): thus the scaffolds consist of alternating amino acids that contain 50% charged residues. The hydrophobic sides must shield themselves from water thus facilitating self-assembly in water, similar to that which has been seen in the case of protein folding. The alanines form overlapping packed hydrophobic interactions in water, a structure that is found in silk fibroin from silkworms and spiders. Once exposed to physiological pH solutions, the hydrophobic side of PuraMatrix forms through compute modeling, a double  $\beta$ -sheet inside of the fiber and a hydrophilic side forms the outside of the nanofibers that interact with water molecules. When the peptides form stable  $\beta$ -sheets in water, they form intermolecular hydrogen bonds along the peptide backbones. On the charged sides, both positive and negative charges are packed together through intermolecular ionic interactions in a checkerboard-like manner. At the concentration used, interwoven nanofibers have a diameter size of  $\sim 10$  nm, yielding nanopores with a range of  $\sim 5$ –200 nm in diameter.<sup>9–11</sup> Puramatrix was poured 30  $\mu$ l/well of a 1% (w/v) distilled water solution, soaked in PBS and allowed to self-assemble at 37° for 30', rinsed 3 times with PBS to wash away any acid residue and dried in laminar hood for 1 hour.

### 5.1.1. Coating Procedure

A laminin coating was chosen because of its widespread use in tissue engineering of the nervous system tissue engineering applications.<sup>46,47</sup> The following substrates were tested with and without coating in order to investigate any possible cell adhesion improvement given by a biomaterial surface treatment (coating with mouse laminin solution at 3  $\mu$ g/cm<sup>2</sup> final concentration): PLLA, PLGA 50:50, PLGA 75:25, PCLA, collagen I, collagen IV and PuraMatrix (RADA16). After leaving the coating solution on top of each scaffold the same protocol of the laminin substrate alone was used.

### 5.2. Cell Maintenance and Seeding

Neural precursor cultures were established and expanded as previously described.<sup>42, 48</sup> In this study, neural precursors isolated from the sub ventricular zone (SVZ) of an 8-week old CD-1 albino mouse striata, at passage 10, were used. Cell proliferation was performed in NS-A serum-free medium (Euroclone, Irvine, UK), in the presence of basic fibroblast growth factor ( $\beta$ FGF) and epidermal growth factor (EGF) at final concentrations of 10 ng/ml and 20 ng/ml. The medium without growth factors was also used as a basal medium. Bulk cultures were generated by mechanically dissociating neurospheres and plating cells in untreated flasks at the appropriate density ( $1 \times 10^4$  cells/cm<sup>2</sup>) every 4–5 days in the same growth medium. Cell counting and viability was performed at every passage, using trypan blue exclusion. Cells were seeded onto different flat substrates into 24 multi-well plates two days

after the last dissociation procedure at a plating density of  $15 \times 10^3$  cells/cm<sup>2</sup> in 20  $\mu$ l of control medium. This timing was adopted to maximize the percentage of stem cells at the starting time of the experiment: indeed at that point in time, due to the selective cell culture protocol adopted, a large fraction of late progenitor, differentiating glia and neurons composing the neurospheres have spontaneously died by two days after last dissociation, while at the same time, new neurospheres (with their heterogeneous cell state population) have not yet formed. Every tested substrate had a surface area of 1 cm<sup>2</sup>. After a pre-adhesion step of 30 minutes at +37°C, medium supplemented with  $\beta$ FGF (10 ng/ml) was added to enhance neuronal progeny differentiation. After 2 days, the medium was shifted to control medium with Ciliary Neurotrophic Factor (CNTF) (20 ng/ml) and Brain Derived Neurotrophic Factor (BDNF) (20 ng/ml) to pursue the neuronal population maturation.<sup>49</sup> At last, a further shift to a control medium containing Leukemia Inhibitory Factor (LIF) (20 ng/ml) and BDNF to promote survival and glial cell maturation<sup>50</sup> in mouse NSCs was performed. The cells were fed every three days with the same fresh culture medium.

For each scaffold, coated and uncoated, a substrate of 1 cm<sup>2</sup> area, without any cells seeded on it, was exposed to the same culture conditions for 28 days (CONTROL I).

### 5.3. Cell Viability Assay

To assess the viability of NSCs seeded on the surface of scaffolds made of various scaffolds, a well-characterized<sup>51</sup> quantitative method, the 3-(4,5-dimethylthiazol-2-yl)-2,5 diphenyl tetrazolium bromide test (MTT Sigma, St. Louis, Missouri), was used. On day 1, 3, 7, and 14 after plating, MTT (5 mg/ml MTT stock solution in PBS) was added to the culture medium in a ratio of 1:100. After an hour incubation at +37°C, the MTT solution was removed and the insoluble formazans crystals were dissolved by soaking them for 15 min in 250  $\mu$ l of dimethylsulfoxide (DMSO). The absorbance was measured by using a Vmax microplate reader (Molecular Devices, Sunnyvale, CA) at a wavelength of 550 nm. Due to the action of the DMSO, some biomaterials partially dissolved during the removal of the insoluble formazans. Therefore, to verify any possible bias in the absorbance measurements, we repeated the same procedure twice for all the biomaterials tested without cells. No significant differences between any of the tested scaffolds and the same DMSO alone could be detected (data not shown).

For this viability test the direct proportional linearity between the optical density and the viability/metabolic activity of the cell populations was assessed by verifying the linearity of 5 different standard curves at 6 increasing cell concentrations, ranging from  $5 \times 10^3$  to  $5 \times 10^5$  per well (data not shown). Results shown in this study are expressed as a percentage of the corresponding

initial population (CONTROL II, cells seeded on Matrigel coated wells right before each multi-well plating and tested 2 hours after plating). These cultures were also kept for 28 days (results not shown).

#### 5.4. Immunocytochemistry

Neuronal and glial differentiation was assessed in cultures seeded onto different scaffolds and exposed to cytokines and neurotrophic factors at the end of days 7 and 14. The cell type composition was analyzed by double and single immunostaining with lineage-specific antibodies. To stain for neuronal, astroglial and progenitor cells, cells were fixed for 20 min in 4% paraformaldehyde in PBS, pH 7.4, washed, and incubated for 120 min at room temperature with PBS/0.1% Triton-X-100, containing 10% normal goat serum. For oligodendroglial assessments, the previous procedure was followed without Triton-X-100 (no permeabilization step). Primary antibodies used were Mouse anti-Nestin (1:150, Chemicon, Temecula, CA), rabbit anti- $\beta$ -Tubulin (1:500, Covance, Berkeley, CA), mouse anti-Glial Fibrillary Acidic Protein (1:200, Chemicon), mouse anti-Galactocerebroside (1:150, Chemicon). After thorough washing, cultures were incubated for 40 minutes at room temperature with secondary ALEXA 488 goat anti-mouse (1:1000 Molecular Probes, Eugene OR) and CY3 AffiniPure F(ab')<sub>2</sub> Fragment Goat Anti-Rabbit IgG antibodies (1:100 Jackson Immuno Research, West Grove, PA), washed, and counterstained with DAPI (Molecular Probes) and viewed under a Nikon TE300 microscope. Quantitative analysis was performed by counting 300–900 cells/well in, depending on cell concentration, 4–15 non overlapping fields that were randomly chosen.

#### 5.5. Atomic Force Microscope (AFM)

The AFM images were collected using a Nanoscope III (Digital Instruments, Santa Barbara, CA) in tapping mode. The tip used was a force modulation etched silicon probe (Veeco Metrology, Sunnyvale, CA) and had a spring constant of 1–5 N/m, a resonance frequency of 60–100 kHz, a nominal tip radius of curvature 5–10 nm, and a cantilever length of 225  $\mu$ m. The scanning parameters were usually as follows: RMS amplitude before engaging the tip 1.0–1.2 V, integral gain 0.2–0.8 and proportional gain 0.4–1.6.

The set point was usually 0.6–1.0 V and the scanning speed ranged from 1.5 Hz to 0.5 Hz. The resolution of the AFM scans were 512  $\times$  512 pixels and the images size scanned ranged from 100  $\mu$ m to 5  $\mu$ m. Before scanning with AFM, cells and scaffolds were fixed 21 days after plating for 20 min in 4% paraformaldehyde in PBS, pH 7.4, washed in distilled water, stored at +4° and dried 30' min before use.

**Acknowledgments:** We thank Dan Andersen, Jason Burdick, and Robert Langer for their helpful discussions and technical advice, Angus Hucknall for his critical

review of the all manuscript. Fabrizio Gelain gratefully acknowledges the support of a fellowship from Fondazione Centro San Raffaele del Monte Tabor, Milan, Italy.

#### References and Notes

1. S. Ceccatelli, P. Ernfors, M. J. Villar, H. Persson, and T. Hokfelt, *Proc. Nat. Acad. Sci. U.S.A.* 88, 10352 (1991).
2. Ramony S. Cajal. Degeneration and Regeneration of the Nerve System. Hafner, New York (1928/1991).
3. C. E. Schmidt and J. B. Leach *Annu. Rev. Biomed. Eng.* 5, 293 (2003).
4. J. H. Philip and F. H. Gage, *Nature* 407, 963 (2000).
5. A. Blesch, P. Lu, and M. H. Tuszynski, *Brain Res. Bull.* 57, 833 (2002).
6. A. Atala and R. P. Lanza, *Methods of Tissue Engineering*. Boston, Academic Press (2002), pp. 1135.
7. Y. D. Teng, E. B. Lavik, X. Qu, K. I. Park, J. Ourednik, D. Zurakowski, R. Langer, and E. Y. Snyder. *Proc. Nat. Acad. Sci. U.S.A.* 99, 3024 (2002).
8. K. I. Park, Y. D. Teng, and E. Y. Snyder, *Nat. Biotech.* 20, 1111 (2002).
9. S. Zhang, T. Holmes, C. Lockshin, and A. Rich, *Proc. Nat. Acad. Sci. U.S.A.* 90, 3334 (1993).
10. S. Zhang, T. Holmes, M. DiPersio, R. O. Hynes, X. Su, and A. Rich, *Biomater.* 16, 1385 (1995).
11. T. C. Holmes, S. de Lacalle, X. Su, G. Liu, A. Rich, and S. Zhang, *Proc. Natl. Acad. Sci. U.S.A.* 97, 6728 (2000).
12. J. Kisiday, M. Jin, B. Kurz, H. Hung, C. Semino, S. Zhang, and A. J. Grodzinsky, *Proc. Natl. Acad. Sci. U.S.A.* 99, 9996 (2002).
13. M. A. Bokhari, G. Akay, S. Zhang, and M. A. Birch, *Biomater.* 26, 5198 (2005).
14. R. Ellis-Behnke, Y. X. Liang, S. W. You, D. Tay, S. Zhang, K. F. So, and G. Schneider. *Proc. Natl. Acad. Sci. U.S.A.* 103, 5054 (2006).
15. M. E. Davis, P. C. H. Hsieh, T. Takahashi, Q. Song, S. Zhang, R. D. Kamm, A. J. Grodzinsky, P. Anversa, and R. T. Lee, *Proc. Nat. Acad. Sci. U.S.A.* 103, (In press)
16. S. Zhang, F. Gelain, and X. Zhao. *Semin. Cancer Biol.* 15, 413 (2005).
17. G. A. Silva, C. Czeisler, K. L. Niece, E. Beniash, D. A. Harrington, J. A. Kessler, and S. I. Stupp, *Science* 303, 1352 (2004).
18. L. E. Niklason and R. S. Langer, *Transpl. Immunol.* 5, 303 (1997).
19. D. G. Wallace and J. Rosenblatt, *Adv. Drug. Deliv. Rev.* 28, 1631 (2003).
20. D. Chafik, D. Bear, P. Bui, A. Patel, N. F. Jones, B. T. Kim, C. T. Hung, and R. Gupta, *Tissue Eng.* 9, 233 (2003).
21. L. Qian and W. M. Saltzman, *Biomater.* 25, 1331 (2004).
22. L. Lu, S. J. Peter, M. D. Lyman, H. L. Lai, S. M. Leite, J. A. Tamada, S. Uyama, J. P. Vacanti, R. Langer, and A. G. Mikos, *Biomater.* 21, 1837 (2000).
23. T. Freier, C. Kunze, C. Nischan, S. Kramer, K. Sternberg, M. Sass, U. T. Hopt, and K. P. Schmitz, *Biomater.* 23, 2649 (2002).
24. J. J. Yoon and T. Park, *J. Biomed. Mater. Res.* 55, 401 (2001).
25. S. Akiyama, K. Yamada, M. Haralson and, J. R. Hassel, *Fibronectin and Fibronectin Fragments*. New York Press (1995).
26. B. A. Reynolds and S. Weiss, *Science* 255, 1707 (1992).
27. A. L. Vescovi and E. Y. Snyder, *Brain. Pathol.* 9, 569 (1999).
28. R. Timpi and J. C. Brown, *Bioessays* 18, 123 (1996).
29. T. Sasaki, R. Fassler, and E. Hohenester, *J. Cell Biol.* 164, 959 (2004).
30. R. J. Schaner, N. D. Martin, T. N. Tulenko, I. M. Shapiro, N. A. Tarola, R. F. Leichter, R. A. Carabasi, and P. J. Dimuzio, *J. Vasc. Surg.* 40, 146 (2004).
31. R. A. Hopper, K. Woodhouse, and J. L. Semple, *Ann. Plast. Surg.* 51, 598 (2003).

32. S. Yoshii, M. Oka, M. Shima, A. Taniguchi, and M. Akagi, *J. Biomed. Mater. Res. A* 67, 467 (2003).
33. G. Lundborg, *Handchir Mikrochir Plast Chir.* 36, 1 (2004).
34. M. D. Pierschbacher and E. Ruoslahti, *Nature* 309, 30 (1984).
35. A. Hautanen, J. Gailit, D. M. Mann, and E. Ruoslahti, *J. Biol. Chem.* 264, 1437 (1989).
36. M. Huber, P. Heiduschka, S. Kienle, C. Pavlidis, J. Mack, T. Walk, G. Jung, and S. Thanos, *J. Biomed. Mater. Res.* 41, 278 (1998).
37. J. P. Ranieri, R. Bellamkonda, E. J. Bekos, T. G. Vargo, J. A. Gardella Jr., and P. Aebischer, *J. Biomed. Mater. Res.* 29, 779 (1995).
38. S. Pluchino, A. Quattrini, E. Brambilla, A. Gritti, G. Salani, G. Dina, R. Galli, U. Del Carro, S. Amadio, A. Bergami, R. Furlan, G. Comi, A. L. Vescovi, and G. Martino, *Nature* 422, 688 (2003).
39. J. L. McBride, S. P. Behrstock, E. Y. Chen, R. J. Jakel, I. Siegel, C. N. Svendsen, and J. H. Kordower, *J. Comp. Neurol.* 475, 211 (2004).
40. K. Chu, M. Kim, K. I. Park, S. W. Jeong, H. K. Park, K. H. Jung, S. T. Lee, L. Kang, K. Lee, D. K. Park, S. U. Kim, and J. K. Roh, *Brain. Res.* 1016, 145 (2004).
41. X. M. Xu, V. Guenard, N. Kleitman, and M. B. Bunge, *J. Comp. Neurol.* 351, 145 (1995).
42. A. Gritti, R. Galli, and A. L. Vescovi, *Protocols for Neural Cell Culture* Humana Press, Totowa, NJ (1999), 3rd edn.
43. M. C. Tate, D. A. Shear, S. W. Hoffman, D. G. Stein, D. R. Archer, and M. C. LaPlaca, *Cell. Transplant.* 11, 283 (2002).
44. T. T. Ngo, P. J. Waggoner, A. A. Romero, K. D. Nelson, R. C. Eberhart, and G. M. Smith, *J. Neurosci. Res.* 72, 227 (2003).
45. Y. Cha and C. G. Pitt, *Biomater.* 11, 108 (1990).
46. C. L. Vleggeert-Lankamp, A. P. Pego, E. A. Lakke, M. Deenen, E. Marani, and R. T. Thomeer, *Biomater.* 25, 2741 (2004).
47. S. P. Massia, M. M. Holecko, and G. R. Ehteshami, *J. Biomed. Mater. Res. A* 1, 177 (2004).
48. A. Gritti, L. Cova, E. A. Parati, R. Galli, and A. L. Vescovi, *Neurosci. Lett.* 185, 151 (1999).
49. H. Song, C. F. Stevens, and F. H. Gage, *Nat. Neurosci.* 5, 438 (2002).
50. R. Galli, S. F. Pagano, and A. Gritti, *Dev. Neurosci.* 22, 86 (2000).
51. J. M. Sargent, *Recent Results Cancer Res.* 161, 13 (2003).

Received: 19 May 2006. Revised/Accepted: 10 September 2006.